Thermochimica Acta, 129 (1988) 29–48
Elsevier Science Publishers B.V., Amsterdam – Printed in The Netherlands

ON THE THERMOCHEMISTRY OF INTERMETALLIC COMPOUNDS

B. PREDEL

Max-Planck-Institut für Metallforschung, Institut für Werkstoffwissenschaften und Institut für Metallkunde der Universität Stuttgart, Seestrasse 92, D-7000 Stuttgart 1 (F.R.G.)

(Received 21 January 1988)

INTRODUCTION

The thermochemistry of intermetallic compounds is relatively old: about 50 years ago, it first blossomed. Many types of crystal structures of compounds of metals were discovered. Weibke and Kubaschewski [1] and many others applied thermochemical investigations to intermetallic phases. This was the great time of accumulation of thermochemical data, and more and more interpretation in connection with the atomic structure of compounds took place. Twenty years ago, Robinson and Bever [2] gave a good synopsis of the concepts and relationships presented until then. Since that time, further investigations have been carried out. Thermochemical data are gaining increasing importance in the search for materials which, at high temperatures, show high strength and corrosion resistance: more and more intermetallic phases are coming into view. Thermochemical data not only yield information about the thermic stability but also, in general, an understanding of the bonding conditions and the structure. In doing so, also ways ought to be indicated by which the properties of the materials can be purposefully optimized.

EXPERIMENTAL METHODS

The principal methods for the determination of thermochemical data have not changed in the last decades. The partial Gibbs free energies of formation are primarily determined by measuring the e.m.f. of suitable galvanic cells or by partial vapor pressure measurements. For determination of the enthalpies of formation of intermetallic phases, solution calorimetry is primarily used. Only the practical method has been varied in different cases. The range of the investigations in many cases during the last years has been extended to

---

Dedicated to Professor Oswald Kubaschewski in honour of his contribution to thermochemistry.

higher temperatures. Furthermore, the progress in analytics as well as in electronic process control and data acquisition is becoming noticeable in so far as results with a higher degree of accuracy can now be attained. Some fundamental problems still remain. Only a few examples will be mentioned here.

The e.m.f. method according to J. Hertz

Figure 1 shows the principle of the measuring arrangement [3]. CaF_2 is used as electrolyte in contact with a Ni/NiO electrode. The method of measurement in the Cu/Ca system will be illustrated here. The Cu and Ca electrodes are formed as pin-points. The arrangement is placed in an argon atmosphere with an extremely low oxygen content (10^{-15} Pa).

With the aid of a current source, the cell Fe–CaF_2–NiO/Ni is polarized. Liquid or solid Ca—depending on the temperature—is precipitated at the Fe pin-point. Fe does not react with Ca; thus one obtains a Ca electrode.

Analogously, Ca can precipitate at the Cu pin-point. Ca reacts with Cu to form a liquid or a solid alloy, dependent on temperature and concentration. The e.m.f. between the Ca electrode and the Ca–Cu electrode complies with the partial Gibbs free energy of Ca in the alloy formed at the Cu pin-point.

The alloy composition, however, cannot be determined. Statements are only possible if a two phase alloy is present at the Cu pin-point. The e.m.f. is followed during the proceeding depolarization. The two phase regions which are visible as hold ranges in the e.m.f.–time curve can be identified from the phase diagram. This method is simple, and a quick investigation of the entire concentration range is possible. Prerequisites for its applications are: (1) one alloy compound has to function as the cation of the electrolyte; (2) the phase diagram has to be known with great precision.

Calorimeter

Kleppa has determined the formation enthalpies of a series of intermetallic compounds by solution calorimetry (e.g. ref. 4). He used a twin

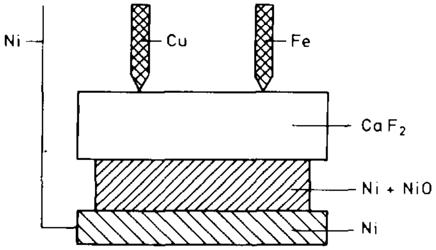

Fig. 1. Principle of the measuring arrangement of the e.m.f. method according to Hertz [3].

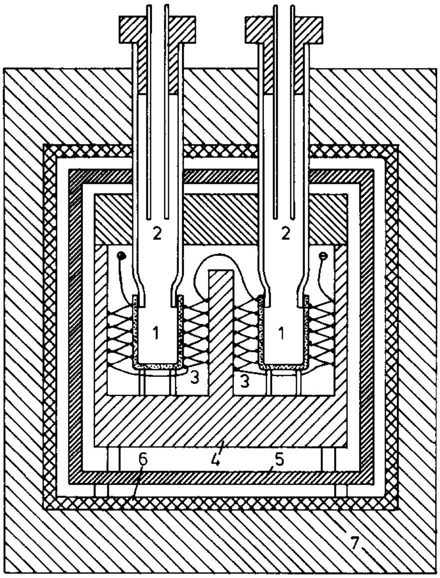

Fig. 2. Twin calorimeter according to Kleppa [5]. 1, Sample crucibles; 2, manipulation tubes; 3, thermopile; 4, calorimeter block; 5, inner shield; 6, heating element; 7, thermal insulation.

calorimeter [5] (Fig. 2). The compounds are dissolved in liquid tin. From the solution enthalpy obtained in this way and the solution enthalpies of the pure components, the formation enthalpy results immediately.

In some cases, the hitherto determined thermodynamic data are sufficient to obtain a general view of the factors which are responsible for the stability of intermetallic phases.

FACTORS AFFECTING THE THERMODYNAMIC STABILITY OF SOLID ALLOYS

Concerning the formation of intermetallic phases, rather different factors are of influence. In general, the interatomic bonds are changed. If one component is inclined to donate electrons while the other one is prone to accept them, an electron transfer may easily take place. A more-or-less strong ionic bonding fraction occurs. For compounds with a considerable ionic character, Pauling [6] has proposed the following relationship between the formation enthalpy and the difference of the electronegativities X_A–X_B

$$\Delta H^F(\text{kcal g-atm}^{-1}) = -23.07(X_A - X_B)^2$$

More-or-less, this seems to hold true.

In many cases, the change of the bonding conditions cannot be comprehended so easily. In addition, as we will see, other factors can be of influence. The part of ΔH^{F} which can be solely attributed to bonding changes will be denoted as ΔH_{B}.

In 1934, Hume-Rothery [7] indicated that the difference of the atomic volumes of the components affects the stability of solid solutions. For intermetallic phases, the difference of the atomic radii can result in lattice distortion, which appears in the enthalpy balance of the formation of the compound as lattice distortion or misfit fraction ΔH_{M}.

Finally the crystal structure of the components is not always the same one as that of the intermetallic phase or of the solid solution. The difference can yield a contribution ΔH_{T} (T = transformation) to the entire formation enthalpy ΔH^{F}. All together, for solid solutions, but also for intermetallic compounds we can write [8]

$$\Delta H^{\mathrm{F}} = \Delta H_{\mathrm{B}} + \Delta H_{\mathrm{M}} + \Delta H_{\mathrm{T}}$$

An analogous formula is valid for the splitting-up of the excess entropy ΔS^{ex} and also holds for the solid as well as for the liquid state [9].

As a simple example, in Fig. 3b the maximal formation enthalpies of solid solutions of some binary Cu and Au systems, respectively, as a function of the relative difference d of the atomic volumes are plotted. Only systems with a demixing tendency, that is with positive ΔH^{F}, have been chosen. By this, specific structural and bonding peculiarities are largely eliminated. The influence of the misfit energy is most distinct. Note that the ordinate intercept complies with the average bonding fraction of the series of systems chosen. In this simple case, it has approximately the same value in the liquid and in the solid alloys.

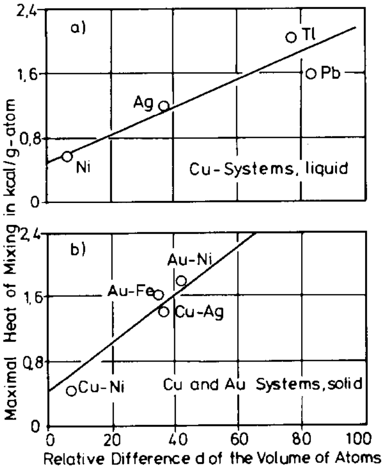

Fig. 3. (a) Maximum mixing enthalpies of liquid Cu alloys as a function of the mean atomic volumes. (b) Maximum formation enthalpies of solid solutions with Cu and Au as one of the components.

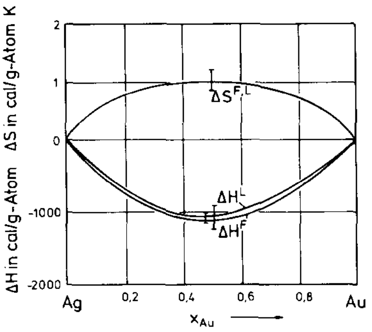

Fig. 4. Mixing enthalpies ΔH^L and mixing entropies ΔS^L of liquid as well as formation enthalpies ΔH^F and formation entropies ΔS^F of solid Ag–Au alloys as a function of the atomic fraction [9,10].

A peculiar case is given in the Au–Ag system. Here, the crystal structures of the components as well as of the solid solutions are equal and this is also almost true for the atomic radii. As can be seen from Fig. 4 the mixing enthalpies of the liquid and the formation enthalpies of the solid solutions are equal within the margins of experimental errors. The same is true for the mixing entropies in the liquid and solid states.

Another extreme case is present in the In–Sn system [11]. The atomic radii are approximately equal. They only differ by 0.6%, and misfit energy is negligible. In the liquid state, the mixing enthalpy is small (see Fig. 5). This hints at the assumption that on the formation of solid solutions the change of the bonding conditions is very small. The formation enthalpy is linearly

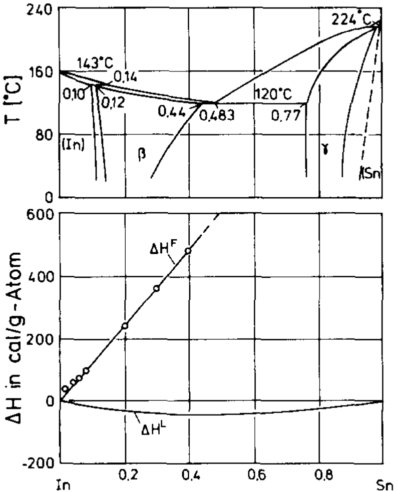

Fig. 5. Phase diagram of the In–Sn system as well as mixing enthalpies [8] and formation enthalpies [12,13] of liquid and solid In–Sn alloys, respectively.

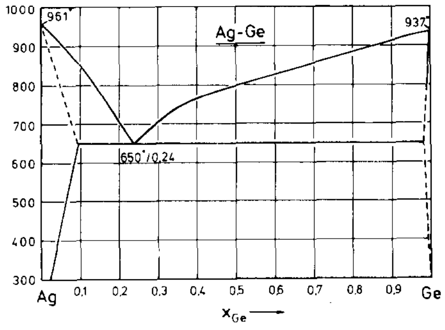

Fig. 6. The Ag–Ge phase diagram [14].

dependent upon the concentration. This is connected with the fact that In and Sn do not have the same structure. The α and β solid solutions are tetragonally face centered; α with $c/a > 1$ and β with $c/a < 1$, whereas the deviation from $c/a = 1$ is in both cases very small. The transformation enthalpy $\alpha \rightarrow \beta$ amounts to $\Delta H_T = 1$ cal g-atm^{-1}. For our purposes, α and β can be regarded energetically as a contingent solid solution region with an approximately cubic fcc lattice. Therefore, as already mentioned $\Delta H_B \approx 0$ and $\Delta H_M \approx 0$. Thus, ΔH^F is determined only by the enthalpy which has to be expended to transform the tetragonal tin into the cubic face centered modification of the solid solution. If ΔH_T^{Sn} is the transformation enthalpy per g-atm, we will have to write

$$\Delta H^F = x_{Sn} \cdot \Delta H_T^{Sn}$$

Thus, ΔH^F is linearly dependent on the mole fraction, as experimentally confirmed. If the ΔH^F–x_{Sn} straight line is extrapolated to $x_{Sn} = 1$, the value ΔH_T^{Sn} is found. The result is [8]

$$\Delta H_T^{Sn}(\text{tetr.} \rightarrow \text{fcc}) = 1.31 \text{ kcal g-atm}^{-1}$$

This is the enthalpy of transformation for the hypothetical transition of the stable white tin into a face centered cubic modification.

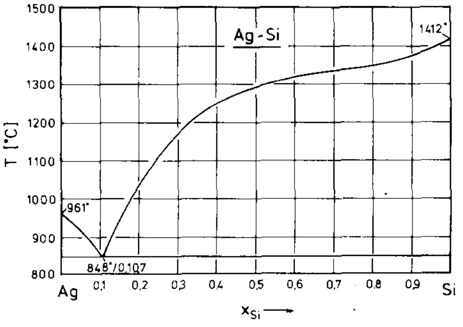

Fig. 7. The Ag–Si phase diagram [14].

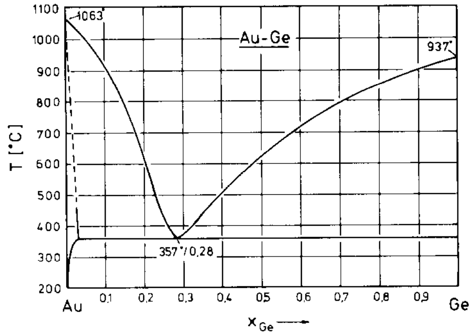

Fig. 8. The Au–Ge phase diagram [14].

In this way, it has been possible to obtain transformation enthalpies of a series of hypothetical phases of elements [9]. So, e.g. the enthalpy of transformation of Ge into a hypothetical fcc modification amounts to ΔH_T^{Ge} (diamond → fcc) = 13 kcal g-atm^{-1}. Such high transformation enthalpies can exert considerable influence on the stability of intermetallic phases, e.g. in the Ag–Ge system no stable Hume-Rothery phase is found (Figs. 6–9). The same is true for the systems Ag–Si, Au–Ge and Au–Si.

After this short survey of the most important factors determining the formation enthalpy of a solid alloy, some groups of intermetallic compounds will now be considered; first superlattice phases which are, as is well known, closely related to solid solutions.

SUPERLATTICE PHASES

If, in a system, solid solutions occur which exhibit negative formation enthalpies, then, if there is a tendency to compound formation, at suffi-

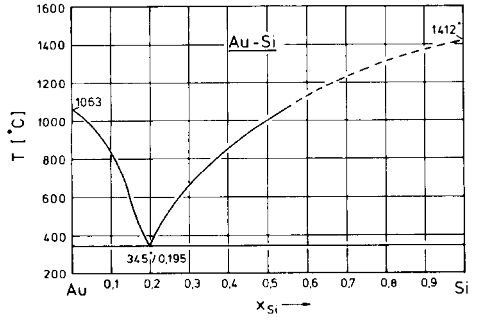

Fig. 9. The Au–Si phase diagram [14].

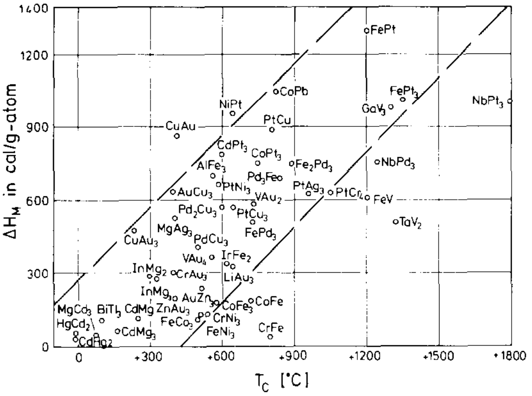

Fig. 10. On the correlation between the lattice distortion or misfit energy of the disordered solid solutions and the stability of the superlattice phases. T_C = critical ordering temperature as a measure for the stability of the superlattice phases [16].

ciently low temperatures a transition from a randomly statistical distribution of the different kinds of atoms into an ordered one may take place. An interatomic interaction between unlike sorts of atoms which is stronger than the average of the interactions between like kinds of atoms is an absolute prerequisite for the existence of a superlattice.

Additionally, a further factor can be effective at which Hume-Rothery and Powell [15] have hinted: this is the lattice distortion which occurs in substitutional solid solutions, if the atomic radii of the components are not equal—as we have seen. For an ordered distribution of the unequally sized atoms the lattice distortion can be reduced. This, of course, favors the formation of a superlattice phase.

The change of enthalpy on the adjustment of the ordering is known only for a few systems. In order to obtain a general synopsis, the critical ordering temperature T_C will be taken as the measure for the stability of the superlattice phases. If the lattice distortion is largely eliminated at the adjustment of the ordering, a correlation between the lattice distortion enthalpy of the disordered solid solution and T_C is to be expected. In Fig. 10, ΔH_M is plotted against T_C [16]. A correlation is distinctly noticeable. With increasing ΔH_M, in general, T_C also increases.

Naturally only a general trend can be roughly noted here. The broad band of the "milky way" is obviously not only the result of measurement errors but also of specific structural conditions and individual bonding factors.

Again it should be stressed that the reduction of the lattice distortion enthalpy leads towards a superlattice phase only if there is a tendency for compound formation. If this tendency is missing, a reduction of the distortion energy may occur by the separation of the mixture at low temperatures into two phases.

As is well known, this kind of intermetallic phases occurs in the case when the mean valence electron concentration (VEC) is 4, that is it equals that of carbon. They crystallize in the diamond structure with a strictly ordered distribution of the kinds of atoms (the zinc blende structure). Covalent bonding is assumed. In a strict sense, this is only the case if there is no difference between the electronegativities of the components. In the presence of an electronegativity difference, the bondings will be polarized. Obviously, the influence of such an ionic bonding fraction increases with increasing difference of the electronegativities; the value of the formation enthalpy also increases. This can be seen from Fig. 11.

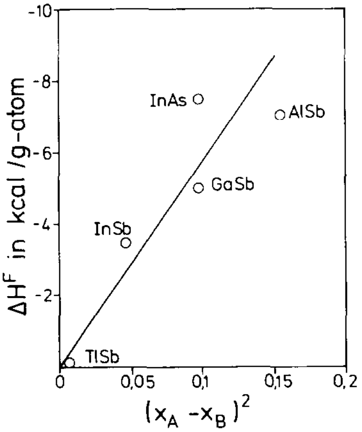

Fig. 11. Formation enthalpies of III–V compounds as a function of the squared electronegativity difference [17].

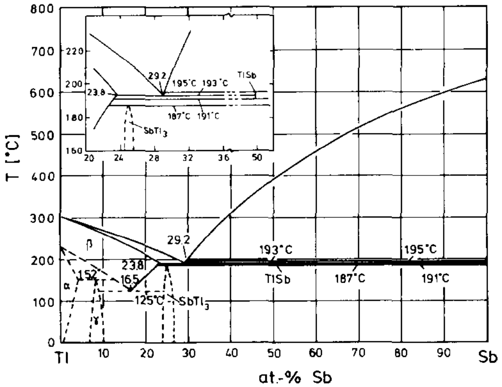

Fig. 12. The Sb–Tl phase diagram [17].

As can be seen from Fig. 11, TlSb has an extremely low enthalpy of formation in comparison with the other III–V compounds depicted here. The phase diagram in Fig. 12 shows that this compound exists only within a very narrow temperature interval of 4 K. Therefore, it is not surprising that it was not possible to get proof of its existence from the X-ray high temperature investigations of El-Boragy, et al. [18]. Still it ought to be mentioned that the enthalpy of formation determined for TlSb is $\Delta H^{\mathrm{F}} = -170 \pm 300$ cal g-atm^{-1} [17]. From this small numerical value it is not surprising that this compound, which is in competition with other phases occurring in the phase diagram, is not stable over a larger temperature range.

HUME-ROTHERY PHASES

The Hume-Rothery phases occur at certain VEC values

	VEC
β-brass type	1.50
γ-brass type	1.62
ε-brass type	1.75

As a rule, they exhibit considerable ranges of homogeneity. Noticeable atomic radii differences impede their formation. In addition to a distinct metallic bonding, at a perceptible electronegativity difference of the components an ionic bonding fraction is present which enhances the stability of these electronic compounds. The ionic bonding fraction may cause the formation of superlattices. As a rule, the β Hume-Rothery phase is the most stable compound among the other compounds of a Hume-Rothery system. In the case of the hitherto investigated β phases the atomic radii difference has no significant importance compared with other influences.

As is well known, the noble metals Cu, Ag and Au, which appear as the monovalent component of the Hume-Rothery phases, are face centered cubic, whereas the β phases are body centered cubic. The enthalpy change connected with this structural difference ought to be small and approximately equal in all three elements. The higher-valent components in the β phases, however, exhibit rather different crystal lattices. Their transmutation into the bcc structure of the β phase is connected with different, in part considerable, ΔH_{T} values. If these values are subtracted from the experimentally obtained ΔH^{F} values, $\Delta H^{\star}$ values result which essentially reflect the change of the bonding conditions which would take place if all higher-valent components started, on alloy formation, from the same initial state, that is from a hypothetical fcc, hcp, or bcc metallic modification. Values of $\Delta H^{\star}$ for some Hume-Rothery phases are plotted in Fig. 13 as a function of $(\Delta x)^2$ [19].

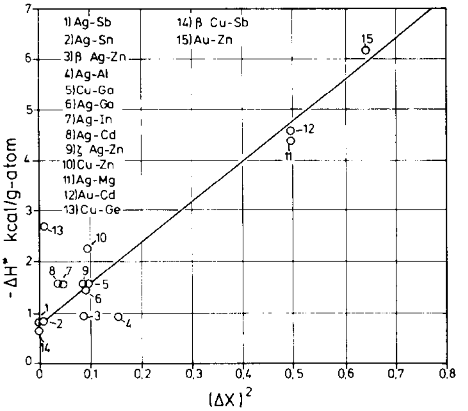

Fig. 13. On the correlation of the "bonding fraction" $\Delta H^{\star}$ of the formation enthalpy ΔH^{F} of β Hume-Rothery phases with the square of the difference of the electronegativities $(\Delta x)^2$ of the components [19].

The influence of a charge transfer and of an ionic bonding fraction connected with it can immediately be seen in Fig. 13.

If there is no charge transfer ($(\Delta x)^2 = 0$), the formation enthalpy of the electronic compounds is relatively small, that is, about 1 kcal g-atm^{-1}. Structural differences between the initial and final states of alloy formation —as already mentioned above—as well as charge transfer at perceptible electronegativity differences can exceed this small value many times over. This will be briefly demonstrated, taking for example the cubic ε Hume-Rothery phases.

METASTABLE HUME-ROTHERY PHASE IN THE Ag–Ge SYSTEM

Looking at Fig. 6 we have seen that no intermetallic phase is present in the system Ag–Ge. If one is solely considering the electronic principles of compound formation, this is surprising. That there is a tendency to form Hume-Rothery phases is indicated by mixing enthalpies of liquid Ag–Ge alloys which have been determined by Ehrlich [20] (Fig. 14). In the region in which in the solid state Hume-Rothery compounds ought to be present,' according to the VEC, a maximal amount of the negative mixing enthalpy is observed. This is also the case in the analogous Ag–Sn system (see Fig. 15). In the Ag–Sn system, however, Hume-Rothery phases occur as the phase diagram in Fig. 16 shows [21]. This is because the transformation enthalpy of Sn is smaller by a factor of ten than that of Ge—in both cases into the most closely packed structure. Obviously the tendency for the formation of Hume-Rothery phases in liquid alloys of so-called Hume-Rothery systems always affects the thermodynamic quantities, even if in the solid state, due

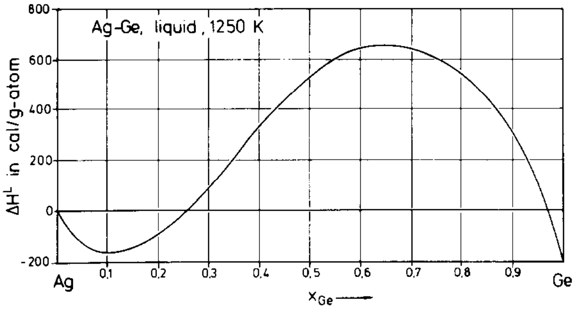

Fig. 14. Mixing enthalpies of liquid Ag–Ge alloys according to Ehrlich [20].

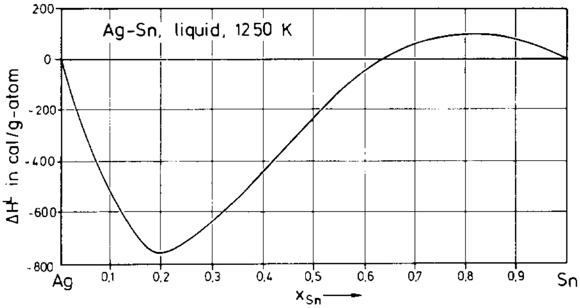

Fig. 15. Mixing enthalpies of liquid Ag–Sn alloys from ref. 10.

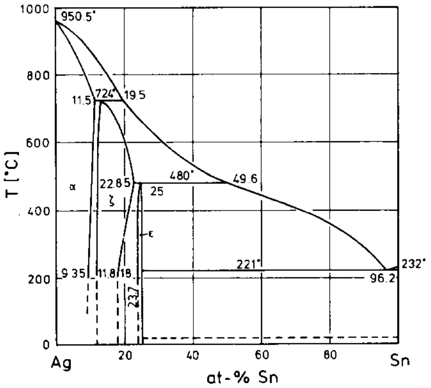

Fig. 16. The Ag–Sn phase diagram [21].

to secondary causes, no Hume-Rothery phases are found. Such a secondary cause is, in the case of the Ag–Ge system, the high transformation enthalpy of Ge from its diamond structure into a closely packed structure of a Hume-Rothery phase. Obviously, this problem of structural difference is not present in the liquid state or, at least, is not so crucial.

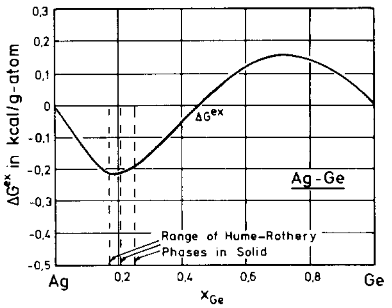

Fig. 17. Integral Gibbs free excess energies of mixing in liquid Ag–Ge alloys calculated from phase equilibria of the phase diagram shown in Fig. 6 according to ref. 14.

This tendency to the formation of Hume-Rothery phases can be shown by considering the thermodynamic properties of the liquid alloys, and also from the phase diagram. As is well known, the excess Gibbs free energy of the liquid alloys can be calculated from the phase equilibria

$$\Delta G^{ex} = \Delta G - \Delta G^{ideal}$$

The result is shown in Fig. 17. The minimum ΔG^{ex} lies in the concentration region $x_{Ge} = 0.2$ where, in the solid state, Hume-Rothery compounds ought to be present. Thus, as is well known, the phase diagram contains more information than can be qualitatively perceived at first sight.

If the bonding and structural conditions of the liquid Ag–Ge alloys with about 20 atm% Ge so distinctly show the inclination for compound formation, it ought to be possible by rapid cooling of these liquid alloys to avoid the nucleation of the solid equilibrium phases and to enable the crystallization of Hume-Rothery phases. Indeed it is possible to produce the hexagonal ε Hume-Rothery phase at a VEC = 1.70. Here, the formation enthalpy of this intermetallic compound is of interest. It amounts to $\Delta H^F = +1.75$ kcal g-atm^{-1} [22]

$$\Delta H^F = +1.75 \text{ kcal g-atm}^{-1}$$

$$\Delta H_T^{Ge} = +13 \text{ kcal g-atm}^{-1}$$

$$\Delta H_B = -1.23 \text{ kcal g-atm}^{-1}$$

$$\begin{aligned} \Delta H^F &= \Delta H_B + \Delta H_M + x_{Ge} \cdot \Delta H_T^{Ge} \\ &= -1.23 + 0 + 0.23 \cdot 13 \\ &= -1.23 + 2.98 \end{aligned}$$

With the aid of the transformation enthalpy of germanium the bonding fraction of the metastable Hume-Rothery phase can be calculated. This bonding fraction is probably arranged among the bonding fractions of other, stable ε Hume-Rothery phases (Fig. 18). In Fig. 18 only those Hume-Rothery phases with hexagonal structure have been considered which, in addition to

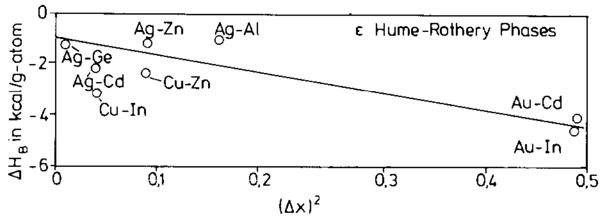

Fig. 18. Bonding part of the enthalpy of formation of ε Hume-Rothery phases as a function of $(\Delta x)^2$.

the monovalent noble metal component, have only such second components whose transformation terms are negligibly small or equal to zero. In addition, in these systems, the lattice misfit enthalpies are also negligible compared with other factors. The bonding fraction of the ε Ag–Ge phase fits well with the ΔH_B–$(\Delta x)^2$ dependence. One sees that the electronegativity difference is small; therefore the bonding fraction is small and thus cannot compensate the transformation term.

LAVES PHASES

Laves phases are the most numerously occurring AB_2 compounds. They have a distinctly metallic bonding. They are characterized by the fact that at a certain relation of the radii, that is 1.225 for atoms assumed to have a spherical shape, the stacking density can be higher than in the most closely packed arrangement of equally sized atoms. When this geometrical prerequisite is fulfilled and no other individual bonding conditions prevail, as e.g. ionic or covalent bondings, then Laves phases can be formed. Then, as we know, the relation of the atomic radii of the components in their respective elementary structures is not the crucial factor, but the relation of the atomic radii of the components within the Laves phase.

In many cases the Laves phases, because of the geometrical conditions, have no noticeable ranges of homogeneity. The three most important types of the Laves phases are

$MgCu_2$	type	cubic
$MgZn_2$	type	hexagonal
$MgNi_2$	type	hexagonal

King and Kleppa [4] investigated the formation enthalpies of a series of Laves phases. They found that at a deviation from the value 1.225 for the ratio of the atomic radii there is a reduction of the amount of the negative formation enthalpy (see Fig. 19). This is because for the adjustment to the correct atomic radii relation, energy for the deformation of the atoms is required.

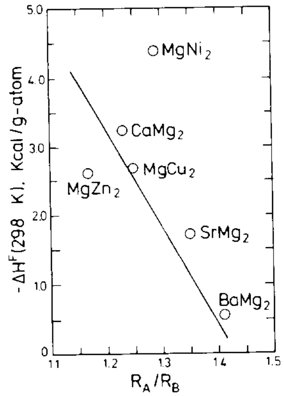

Fig. 19. Formation enthalpies of Laves phases as a function of the ratio of the radii R_A/R_B of the elements in their stable elementary structures [4].

On the other hand the authors established that, if an element of the Laves phase is a transition metal, there is a charge transfer in the course of which not entirely occupied inner electron shells are filled up. In this way an ionic bonding fraction ensues which causes an increase in the mixing enthalpy. Let us look at the $MgNi_2$ phase in Fig. 19 for example. The 3d band of the nickel is only partially occupied [2]. It can be filled up by the electrons of Mg [4]. Wertheim and Wernick [23] have been able to prove by Mössbauer spectroscopy for $CeFe_2$ that 4f electrons of Ce are partially transferred into the d band of Fe. The expense in misfit energy can be compensated by this effect. A large deviation of the atomic radii relation from that characteristic for a Laves phase is obviously tolerated only if one component is a transition metal.

Figure 20 represents the elementary cell of the cubic Laves phase ($MgCu_2$ type structure). The big Mg atoms occupy the sites of the cubic face centered lattice, and half of the sites comply with the centers of the tetrahedral voids.

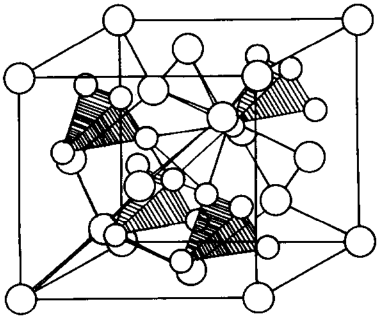

Fig. 20. Elementary cell of the cubic $MgCu_2$ Laves phase. Big spheres = Mg; small spheres = Cu.

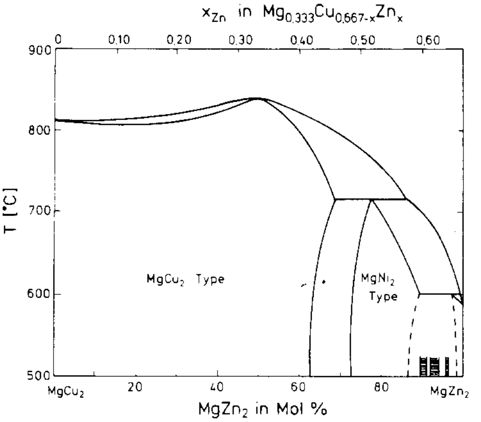

Fig. 21. Quasibinary section $MgCu_2$–$MgZn_2$ [26]. Also drawn in are the stacking variants of the Friauf–Laves–Komura phases [27].

Around the centers of the other tetrahedral voids, respectively, 4 Cu atoms are placed. Both partial lattices penetrate each other without distortion, as Schulze [24] has demonstrated. The intermetallic interaction in the partial lattice of B is decisive for the energetic cohesion of the Laves lattice.

Laves and Witte [25] have pointed at the influence of the valence electron concentration on the structural types of Laves phase. Between $MgCu_2$ and $MgZn_2$, the formation of solid solution takes place, as Fig. 21 shows. The

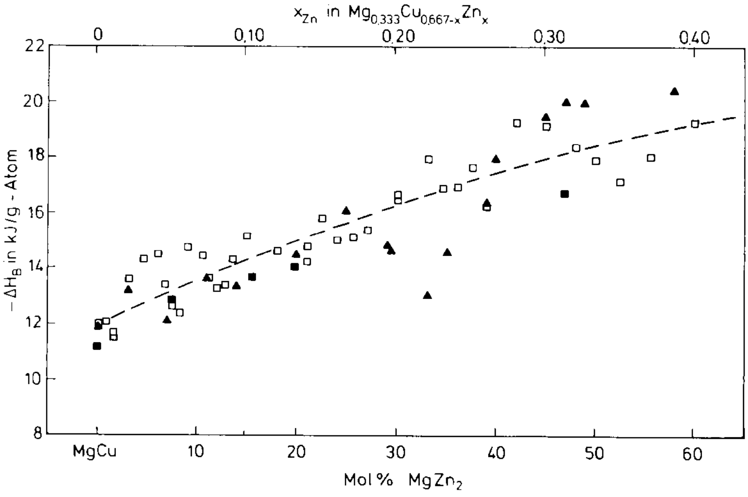

Fig. 22. Formation enthalpies of $MgCu_2$–$MgZn_2$ solid solutions according to refs. 4 (■), 26 (□) and 29 (▲). The formation enthalpies of Cu–Zn solid solutions [28] (- - - - - -) are elevated by the amount of the formation enthalpy of $MgCu_2$.

individual regions with the pertinent Laves phases are shown in Fig. 21. The region of the existence of the cubic phase lies at low VEC values (from 1.33 onward); at higher VEC values (up to 1.5) the $MgZn_2$ type is stable, and all other hexagonal stacking variations lie between them.

In the solid-solution region of the cubic $MgCu_2$ type, formation enthalpies have been determined by King and Kleppa [4]. Following this, measurements in this solid-solution region have been carried out by our group.

On the formation of solid solutions, due to geometrical causes, the Zn atoms go into the partial B lattice, that is the Cu lattice. Therefore Cu–Zn interactions result as they are present in binary Cu–Zn solid solutions. There are no contacts between Mg and Zn atoms and, likewise, none between Cu and Mg. Therefore it is useful to compare the formation enthalpies of the solid solutions of the Laves phases with those of the Cu–Zn solid solutions. In Fig. 22 the concentration dependence of the formation enthalpies of the Cu–Zn solid solutions enhanced by the amount of the formation enthalpy of Mg_2Cu, are shown. It is obvious at first sight that the course of the formation enthalpies of the Laves solid solutions is in agreement with the concentration dependence of the formation enthalpies of the Cu–Zn solid solution. The change of the formation enthalpy by the addition of Zn is largely caused by the interaction between the Cu and the Zn atoms in the B partial lattice of the Laves phases.

The presentation in Fig. 22 suggests that the scattering width of the measurement results is rather considerable. If, however, only one series of measurements, that is the one with the most alloys investigated, is plotted alone, then a curve with some minima and maxima results (see Fig. 23). The

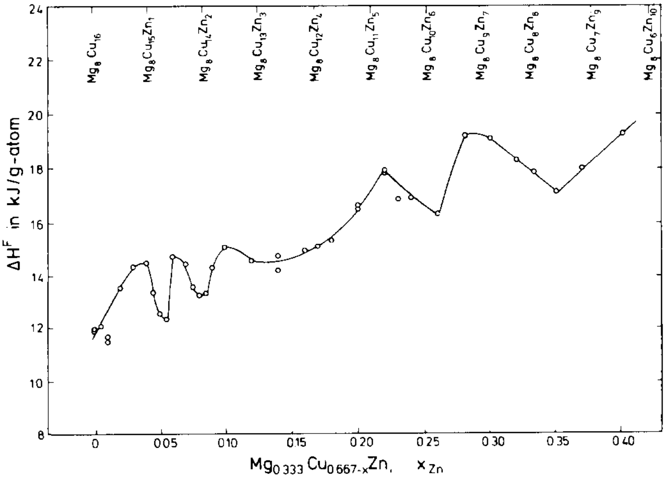

Fig. 23. Formation enthalpies of $MgCu_2$–$MgZn_2$ solid solutions according to ref. 26.

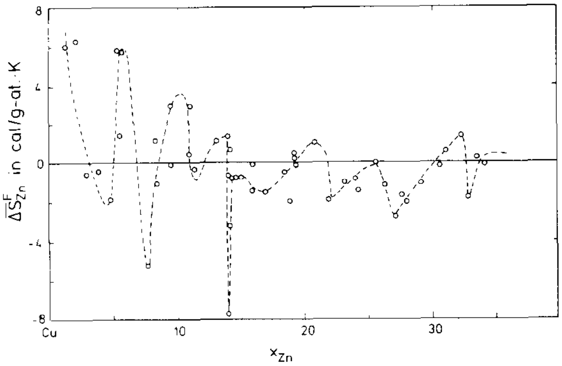

Fig. 24. Partial molar formation entropies of α Cu–Zn solid solutions from refs. 31–33.

minima are positioned at certain stoichiometric compositions, giving a simple regularity if one chooses an elementary cell with eight Mg atoms [26]

Mg_8Cu_{16}
$Mg_8Cu_{15}Zn_1$
$Mg_8Cu_{14}Zn_2$
$Mg_8Cu_{13}Zn_3$
$Mg_8Cu_{12}Zn_4$
$Mg_8Cu_{11}Zn_5$
$Mg_8Cu_{10}Zn_6$
$Mg_8Cu_9Zn_7$
$Mg_8Cu_8Zn_8$
$Mg_8Cu_7Zn_9$
$Mg_8Cu_6Zn_{10}$

At five of these compositions $Mg_8Cu_{16-x}Zn_x$ there are minima in the ΔH^F-concentration curve. It was not possible, however, to confirm by neutron diffraction experiments [31] the presumption that superlattices occur. Anyway X-ray diffraction experiments are not apt to yield evidence in this case because of the similar diffraction abilities of copper and zinc. Here, electronic sublattices are possibly manifesting themselves.

It is remarkable that similar oscillations of thermodynamic quantities have also been found in α Cu–Zn solid solutions [31]. In Fig. 24 the partial formation entropy of zinc in α Cu–Zn solid solutions is plotted as a function of x_{Zn}. The question is whether this curve is the best fit for the measured points for the enthalpy of formation of the Laves phases. Possibly it does, after all, represent reality. There are, indeed, some conformities between the oscillations in the Cu–Zn system and the Cu–Zn placements in the B partial lattices of the Laves phases, if one assumes that the Mg partial lattice exerts no special influence on the $MgCu_2$–$MgZn_2$ solid solutions. Therefore one can operate with an atomic fraction x_{Zn} as it is resulting solely for the B partial lattice. The first two maxima and also further details of the curves are positioned, as Fig. 25 shows), at the same concentrations. Perhaps one should once more after all rethink what the meaning of these oscillations of ΔH^F could be. Above all, still more accurate (and also other

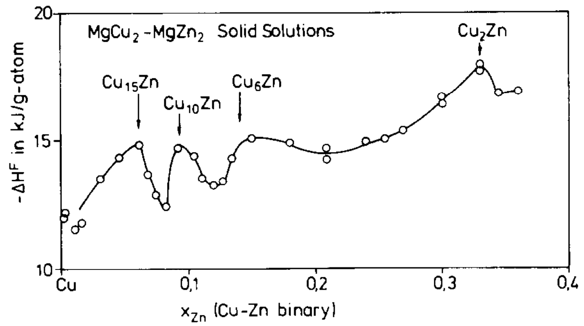

Fig. 25. Comparison of Fig. 23 with Fig. 24. For the $MgCu_2$–$MgZn_2$ solid solutions, x_{Zn} denotes the atomic fraction in the B partial lattice of the Laves phase.

kinds of) experiments need to be undertaken, e.g. exact measurements of the electrical resistivities.

CONCLUDING REMARKS

There is still much work to do in the field of thermochemistry. Carrying out the experiments is often not easy, and model calculations do not always lead to complete success. Therefore, in this study, I have tried to proceed pragmatically.

REFERENCES

1 F. Weibke and O. Kubaschewski, Thermochemie der Legierungen, Springer-Verlag, Berlin, 1943.

2 P.M. Robinson and M.B. Bever, in J.H. Westbrook (Ed.), Intermetallic Compounds, Wiley, New York, 1967.

3 M. Notin, C. Cunat and J. Hertz, Thermochim. Acta, 33 (1979) 175.

4 R.C. King and O.J. Kleppa, Acta Metall., 12 (1964) 87.

5 O.J. Kleppa, J. Phys. Chem., 64 (1960) 1937.

6 L. Pauling, The Nature of the Chemical Bond, Cornell Univ. Press, Ithaca, New York, 3rd edn., 1960.

7 W. Hume-Rothery, G.W. Mabbott and K.W. Channell-Evans, Phil. Trans. R. Soc., A 233 (1934) 1.

8 O. Alpaut and Th. Heumann, Acta Metall., 13 (1965) 543.

9 B. Predel, Thermodynamik und Aufbau von Legierungen—einige neuere Aspekte, Westdeutscher Verlag, Opladen, 1973.

10 R. Hultgren, R.L. Orr, P.D. Anderson and K.K. Kelley, Selected Values of Thermodynamic Properties of Metals and Alloys, Wiley, New York, 1963 (and Supplements).

11 T. Heumann and O. Alpaut, J. Less-Common Met., 6 (1964) 108.

12 O.J. Kleppa, J. Phys. Chem., 60 (1956) 842.

13 F.E. Wittig and P. Scheidt, Z. Phys. Chem. Neue Folge, 28 (1961) 120.

14 B. Predel and H. Bankstahl, J. Less-Common Met., 43 (1975) 191.

15 W. Hume-Rothery and H.M. Powell, Z. Kristallogr., 91 (1935) 23.
16 B. Predel and W. Schwermann and W. Gust, Metall, 25 (1971) 1002.
17 B. Predel and W. Schwermann, Z. Naturforsch., 25a (1970) 877.
18 M. El-Boragy, M. Ellner and B. Predel, Z. Metallkd., 75 (1984) 58.
19 B. Predel and D.W. Stein, Acta Metall., 20 (1972) 681.
20 K. Ehrlich, Inaugeral-Dissertation, Ludwig-Maximilian-Universität, München, Germany, 1965.
21 M. Hansen and K. Anderko, Constitution of Binary Alloys, McGraw-Hill, New York, 1958.
22 G. Schluckebier and B. Predel, J. Less-Common Met., 75 (1980) 55.
23 G.K. Wertheim and J.H. Wernick, Phys. Rev., 125 (1962) 1937.
24 G. Schulze, Z. Electrochemie, 45 (1939) 849.
25 F. Laves and H. Witte, Metallwirtsch., 15 (1936) 840.
26 B. Predel, H. Bencker, W. Vogelbein and M. Ellner, J. Solid State Chem., 28 (1979) 245.
27 Y. Komura, M. Mitarai, A. Nakaue and S. Tsujimoto, Acta Crystallogr., B 28 (1972) 976.
28 R. Hultgren, P.B. Desai, D.T. Hawkins, M. Gleiser, K.K. Kelley and D.D. Wagman, Selected Values of the Thermodynamic Properties of Binary Alloys, ASM, Cleveland, Ohio, 1973.
29 B. Predel and H. Ruge, Mater. Sci. Eng., 9 (1972) 141.
30 M. Ellner and B. Predel, J. Solid State Chem., 30 (1979) 209.
31 B.B. Argent and D.W. Wakeman, Trans. Faraday Soc., 54 (1958) 799.
32 R. Hargreaves, J. Inst. Met., 64 (1939) 115.
33 W.A. Herbenar, C.A. Siebert and O.S. Duffendack, Trans. AIME, 188 (1950) 323.